Packet data transmission in worldwide interoperability for microwave access with reduced peak to average power ratio and out-band distortion using software defined radio

Bathula Siva Kumar Reddy ✉, *B. Lakshmi*

Department of Electronics and Communication Engineering, National Institute of Technology, Warangal – 506004, India
✉ E-mail: bsivakumar100@gmail.com

Abstract: The high peaks of a conventional orthogonal frequency division multiplexing (OFDM) symbol may push the amplifier into the non-linear region, which creates many problems that reduce performance and lead to out of band distortion. In this study, the authors present and analyse four different peak to average power ratio (PAPR) reduction techniques such as phase modulation, rail clipping, sample and hold approach and threshold method for packet data transmission of OFDM on mobile-worldwide interoperability for microwave access system. The performance of each PAPR reduction technique on OFDM system is presented in time and frequency domains separately. Therefore an existing OFDM system can provide an additional CE-OFDM mode with relative ease, particularly for the case of software defined platforms. Nowadays, the behaviour of a communication system has been modified by simply changing its software. This gave rise to a new radio model called software defined radio, in which all hardware components are implemented in software rather than in hardware. For our investigation, GNU radio and universal software radio peripheral N210 are employed as software and hardware platforms, respectively. It is shown that for a high clipping threshold value, the gap between in-band and out-of-band radiations is maintained well.

1 Introduction

Wireless communications is the fastest growing segment of the communications industry and the broadband wireless at the confluence of the most remarkable growth stories of telecommunication industry in recent years. worldwide interoperability for microwave access (WiMAX) [1–3] is an emerging broadband wireless technology based on the IEEE 802.16 standard. The core 802.16 specification is a standard for broadband wireless access systems operating at radio frequencies between 10 and 66 GHz. The WiMAX physical layer (PHY) is based on orthogonal frequency division multiplexing (OFDM) [4–8], however fixed and mobile version of WiMAX have slightly different implementation of the OFDM. Fixed WiMAX (IEEE 802.16) uses 256 inverse fast Fourier transform (IFFT) block size and mobile WiMAX (IEEE 802.16e-2005) [3] uses scalable OFDMA. The inclusion of MIMO antenna techniques along with flexible sub-channelisation schemes, advanced coding and modulation all enable the 802.16e technology to support peak down link data rates up to 63 Mbps per sector and peak up link data rates up to 28 Mbps per sector in a 10 MHz channel [2].

Recently, a multi-carrier technology, OFDM, has been integrated in wireless and wire-line communications because of its immunity to multipath fading/frequency selective fading and impulse noisy channels. A key benefit of orthogonal frequency division multiplexing (OFDM) is that it can be efficiently implemented using the fast Fourier transform (FFT), and that the receiver structure becomes simple since each channel or subcarrier can be treated as narrow-band instead of a more complicated wide-band channel.

Therefore, an OFDM signal is the superimposition of a number of modulated subchannel signals which may produce an extreme peak signal with reference to the average signal level, which gives rise to high peak to average power ratio (PAPR) [9–11]. To deal with this PAPR problem, several techniques have already been developed in the literature for instance coding and tone reservation [12],

clipping/filtering [13], peak windowing [14], partial transmit sequence [15] and receiver correction algorithms [16] such as iterative decoding. As discussed in [17], each one of these distinctive methods provides different quantities of effectiveness and presents different sets of trade-offs that may include reduced spectral efficiency, increased complexity and performance degradation. Among these techniques, clipping and filtering is possibly the simplest PAPR reduction scheme. This scheme directly clips OFDM signals to a predefined threshold and then uses a filter to eliminate the out-of-band radiation. Nevertheless, the filtering operation results in peak regrowth. Hence, iterative clipping and filtering (ICF) is usually needed to suppress the peak regrowth [18]. However, the convergence rate of this method to the desired PAPR becomes very slow after several iterations. Another drawback of ICF is that this technique does not consider combating the in-band distortion.

Recently, in [19] Wang and Luo concentrated their attention on the clipped signals and developed an algorithm called optimised ICF (OICF). In this algorithm, frequency-domain filtering is formulated as an optimisation problem and the optimisation parameters are the filter coefficients. By using the optimal coefficients to weigh the clipped signals, one can minimise the signal distortion under the constraints of PAPR reduction and out-of-band radiation. Therefore OICF is an optimal algorithm, and another attractive advantage of this algorithm is that it only needs about three iterations to converge to the desired signal. However, the optimal filter design needs to solve a convex optimisation problem by using some special software, which has $O(N^3)$ complexity for OFDM systems with N subcarriers.

In this paper, four techniques such as phase modulation [11], rail clipping, sample and hold approach and threshold methods are employed to obtain a constant envelop(CE)-OFDM by clipping the peak amplitudes [20]. In these four techniques, the clipping threshold levels of phase modulation and sample and hold methods are predefined; and rail clipping and threshold techniques are user defined. The resulting CE-OFDM waveform alleviates the

PAPR problem. The threshold levels can be reconfigurable at run time also. This point is further illustrated with experimental results in Section 5 and relevant equations are defined in Sections 2 and 3.

Experimental tests are performed using universal software radio peripheral (USRP) N210 [21], which is a low cost software defined radio (SDR) [22–24] transceiver platform and the GNU Radio free software [25], which is a framework for building real-time signal processing systems as shown in Fig. 1a. In this paper, authors use the USRP N210 for both transmitting and receiving signals. It has a much wider bandwidth, programmable centre frequency, programmable gain and choice of sample rates. Refer to the block shown in Fig. 1b to understand the path of reception of the USRP as it is set up in the lab. The USRPs in the lab have the WBX daughter-card installed which features a programmable attenuator, programmable local oscillator and analog I/Q mixer. This board allows the USRP to receive signals in the range from 50 MHz to 2.2 GHz. The main function of the USRP main board is to act as a digital down-converter. We can consider this as a digital I/Q mixer, sample rate converter and lowpass filter. The samples are then sent to the host PC over a gigabit Ethernet link. The Ethernet cable acts as the interface between the analog RF front-end (USRP N210) and the host PC where all the signal processing is done in software. GNU Radio software is originally a streaming system with no other mechanism to pass data between blocks. Streams of data are a model that work well for samples, bits etc., but are not really the right mechanism for control data, metadata and often, packet structures (at least at some point in the processing chain). The authors of this paper solved a part of this problem by introducing the tag stream. This is a parallel stream to the data streaming. The difference is that tags are designed to hold metadata and control data.

A packet comprises of two sorts of data: user data (also known as payload) and control data [26]. The control data provides the information about source and destination network addresses, error detection codes and sequencing information of user data. Generally, the control data with payload is detected between the packet headers and trailers. Larger packets can be separated in to small packets when necessary and these smaller packets also should be formatted as packets. In this work, packet data transmission is carried out in an OFDM transceiver. The Complete PHY with packet data transmission in OFDM is carried out in GNU Radio with the help of USRP N210.

2 Background

2.1 Non-OFDM system

Consider a non-OFDM or single carrier system with binary phase shift keying (BPSK) modulated symbols as $x(0)$, $x(1)$, $x(2)$, ... with an amplitude level $\pm a$.

Power in each symbol $= a^2$ (peak power)

Average power $= E|x(k)|^2 = a^2$

Hence, in this single carrier system, both peak and average power $= a^2$.

$$\text{Ratio} = \frac{\text{Peak power}}{\text{Average power}} = \frac{a^2}{a^2} = 1 = 0 \text{ dB} \qquad (1)$$

Hence, there is no significant deviation from the mean power level.

2.2 OFDM system

In an OFDM system, let us denote the information symbols as $X(0)$, $X(1)$, $X(2)$, …, $X(N-1)$ with amplitude $\pm a$. These information
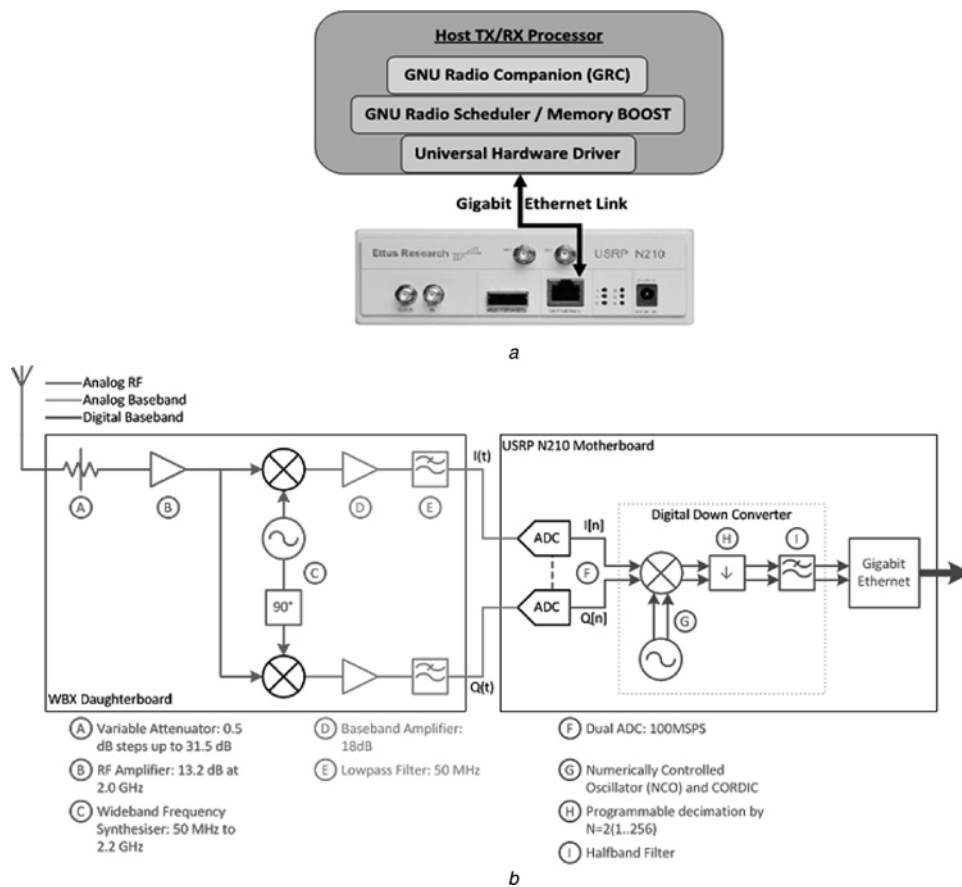

Fig. 1 *Experimental tests are performed using USRP*
a SDR experimental setup with software and hardware
b USRP N210 internal architecture

symbols are loaded on to the subcarriers using IFFT. Hence, the transmitted samples are $x(0), x(1), ..., x(N-1)$, which are the IFFT samples of information symbols $X(0), X(1), ..., X(N-1)$.

A Kth IFFT sample $x(k)$ is defined as

$$x(k) = \frac{1}{N}\sum_{i=0}^{N-1}X(i)e^{j2\pi k_i/N} \qquad (2)$$

Average power $= E|x(k)|^2$

$$= \frac{1}{N^2}\sum_{i=0}^{N-1}E|x(i)|^2 = \frac{1}{N^2}\sum_{i=0}^{N-1}a^2 = \frac{1}{N^2}.a^2.N = \frac{a^2}{N} \qquad (3)$$

at zeroth sample, $x(0)$ is

$$x(0) = \frac{1}{N}\sum_{i=0}^{N-1}X(i) \qquad (4)$$

and $X(0) = X(1) = X(2) = \cdots + X(N-1) = +a$

$$x(0) = \frac{1}{N}\sum_{i=0}^{N-1}a = a \qquad (5)$$

Hence, peak power $= a^2$. Therefore

$$\text{PAPR} = \frac{a^2}{a^2/N} = N \qquad (6)$$

Hence, PAPR in an OFDM system can be significantly higher. Further, the PAPR raises with the number of subcarriers (N). The high PAPR in an OFDM system essentially arises because of the IFFT operation as information symbols across subcarriers can add up to produce a high peak value symbol. For instance in an OFDM system with 512 subcarriers, and BPSK modulation, the PAPR at the output can be as high as 10 dB.

In OFDM system, when the peak deviation about average is significantly high, the signal level moves outside the dynamic linear range. Hence, high PAPR in OFDM results in amplifier saturation results in loss of orthogonality thus leading to inter carrier interference.

Let us denote the collection of data symbols of an OFDM block $X = [X(0), X(1), ..., X(N-1)]$. The discrete-time OFDM symbol $x(n)$ can be obtained by

$$x(n) = \frac{1}{\sqrt{N}}\sum_{k=0}^{N-1}X(k)e^{j2\pi nk/LN}, \quad n = 0, 1, ...LN-1 \qquad (7)$$

where $X(k)$ represents the data symbol carried by the kth subcarrier and L is the oversampling factor. In this paper, the oversampling operation is implemented by zero padding, that is, appending $(L-1)N$ zeros to the end of X to yield $[X(0), X(1), ..., X(N-1), 0, 0, ..., 0]$. For this case, the interval τ in (7) is $[0, LN-1]$.

Assume that $X(k)$ are statistically independent and identically distributed random variables. According to the central limit theorem, the real and imaginary parts of $x(n)$ are Gaussian random variables with zero mean and the same variance σ^2 when N is large (usually $N \geq 64$ [27]). Therefore, its amplitude $|x(n)|$ is Rayleigh distributed, which means the peak power of $x(n)$ can take a value much larger than its average power [19] (page 57). That is to say, the OFDM signal has a large PAPR, which leads to a negative impact on the system performance.

In the ICF method, $x(n)$ is clipped to a predefined threshold by using a soft limiter. The clipped signal $\bar{x}(n)$ is given by

$$\bar{x}(n) = \begin{pmatrix} Ae^{j\phi(n)}, & |x(n)| > A \\ x(n), & \text{otherwise} \end{pmatrix} \qquad (8)$$

where $A > 0$ represents the predefined threshold and $\phi(n)$ is the phase of $x(n)$. The clipping ratio γ is defined as [21]

$$\gamma = \frac{A}{\sqrt{P_{\text{avg}}}} \qquad (9)$$

where P_{avg} is the average power of the signals before clipping. Amplitude clipping leads to in-band distortion and out-of-band radiation. To satisfy the spectral constraint, a filter is required to eliminate the out-of-band radiation. Filtering is applied to the baseband signals in the frequency domain [14], and the filter design is based on a rectangular window with frequency response defined by [18]

$$H_r(k) = \begin{pmatrix} 1, & 0 \leq k \leq N-1 \\ 0, & N \leq k \leq LN-1 \end{pmatrix} \qquad (10)$$

Unfortunately, a side effect of filtering is peak regrowth. Therefore, repeated clipping and filtering is required to suppress the peak regrowth. Nevertheless, the convergence rate of this method to the desired PAPR becomes very slow after several iterations. Another
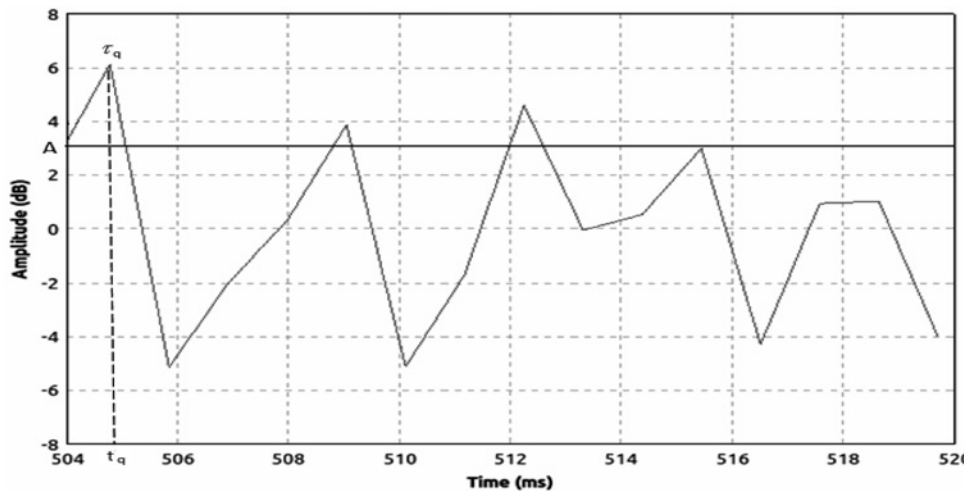

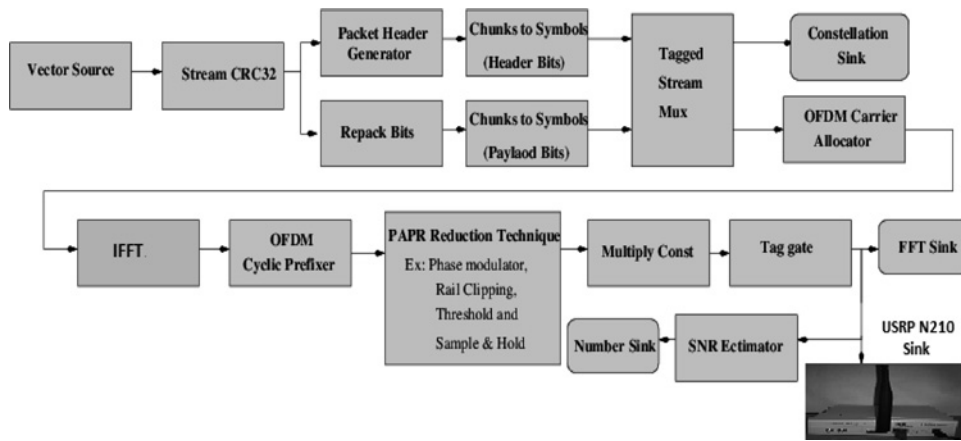**Fig. 2** *Amplitude variation of an OFDM signal*

Fig. 3 *GNU schematic of transmitter section for packet data transmission with USRP N210 Tx*

drawback of ICF is that this technique does not consider combating the in-band distortion.

Recently, a technique called OICF has been proposed in [19], which considers a comprehensive performance in terms of PAPR reduction, error vector magnitude (EVM) and out-of-band radiation. As a result, it can effectively improve the performance of ICF. At each iteration of OICF, the signal is first clipped to the predefined threshold and then an optimised filter is used instead of

the rectangular filter to minimise the clipped signal's EVM under the constraints of PAPR and out-of-band radiation.

3 Analysis of clipping

The amplitude variation of an OFDM signal $x(t)$ is shown in Fig. 2. We observe that the signal exceeding the clipping threshold (A) consists of a
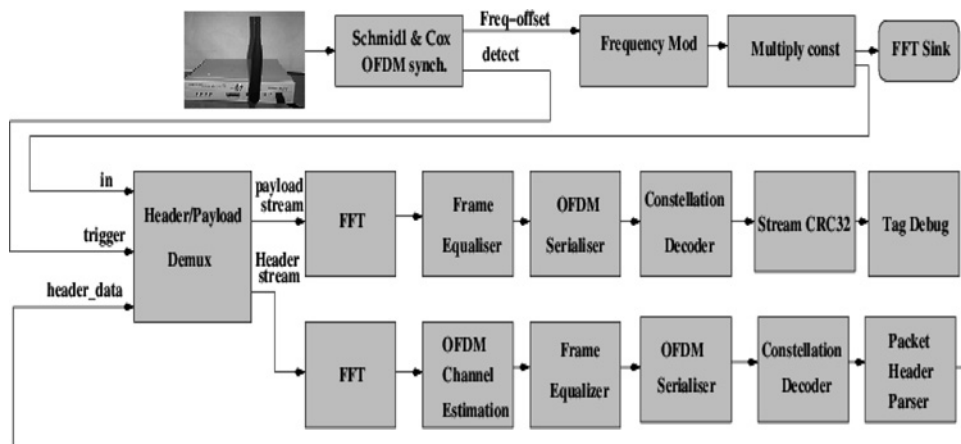

Fig. 4 *GNU schematic of receiver section for packet data transmission with USRP N210 Rx*
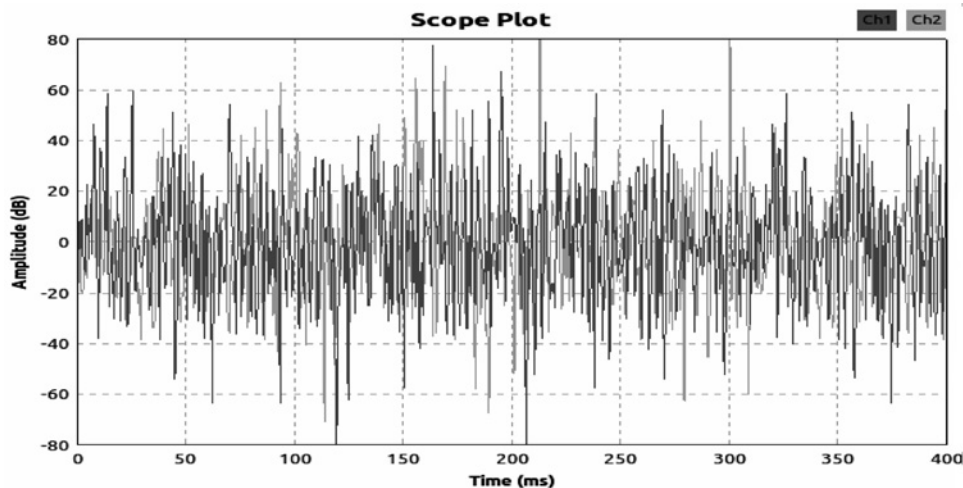

Fig. 5 *Generated OFDM symbol without using any PAPR reduction technique*

series of approximately parabolic pulses. Let's assume that $f_q(t)$ represent the q-th pulse exceeding A as shown in Fig. 2, its maximum amplitude occurs at t_q with pulse duration is τ_q. Then $f_q(t)$ can be defined as

$$f_q(t) = x(t)\text{rect}_{\tau_q}(t - t_q) \tag{11}$$

where $\text{rect}_{\tau_q}(.)$ denotes a rectangular window function as follows

$$\text{rect}_{\tau_q}(t) = \begin{cases} 1, & \dfrac{-t_q}{2} \le t \le \dfrac{t_q}{2} \\ 0, & \text{otherwise} \end{cases} \tag{12}$$
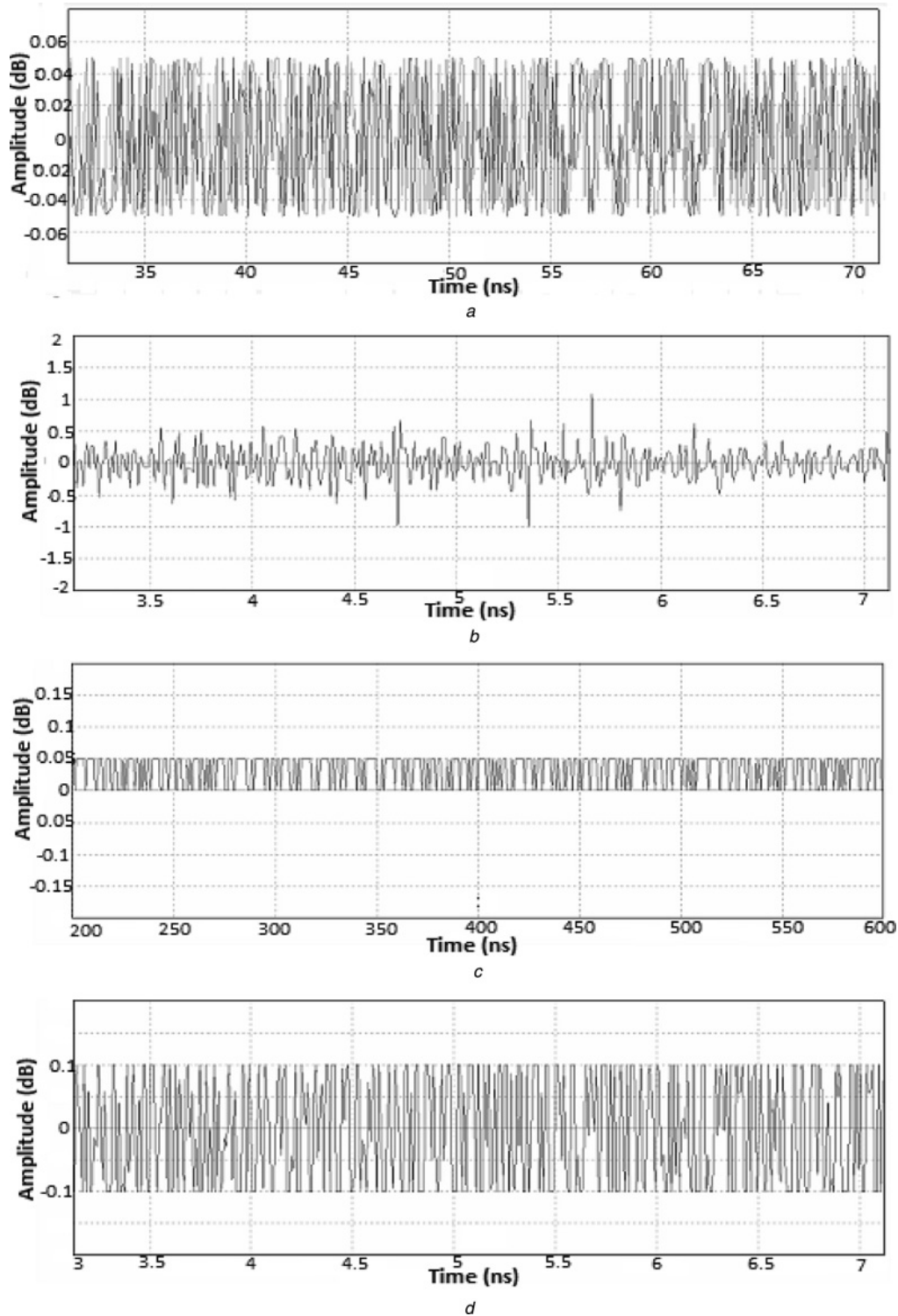

Fig. 6 *OFDM symbol after using PAPR reduction schemes*
a Phase modulation
b Sample and hold
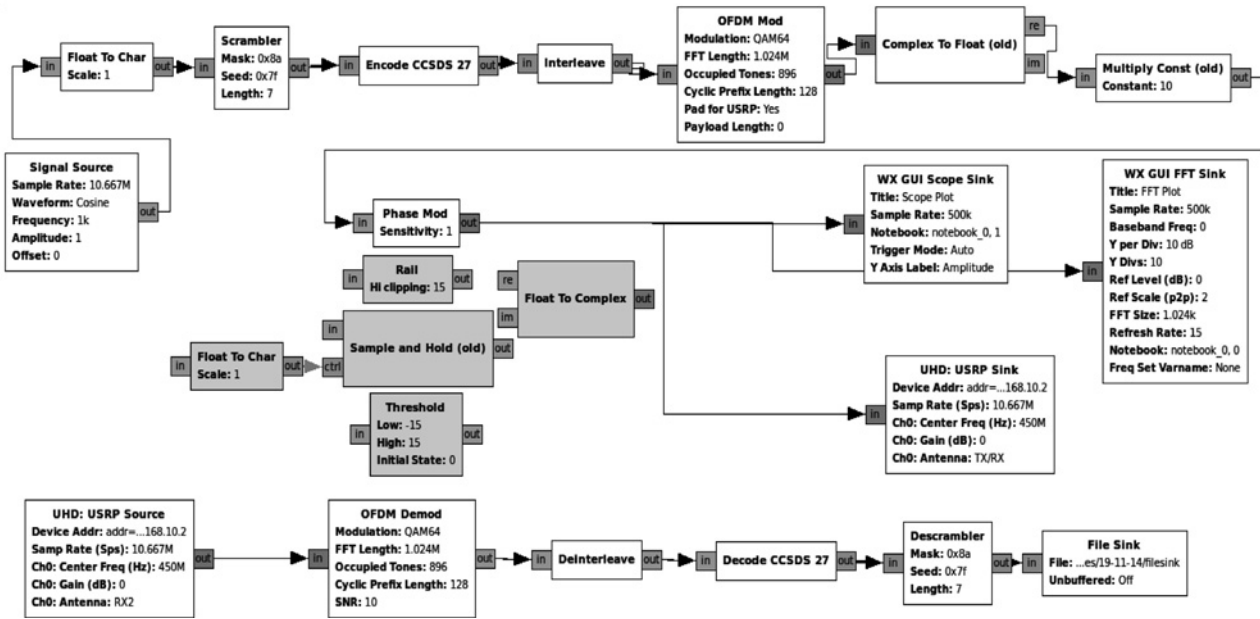*c* Threshold method
d Rail clipping method

Fig. 7 *GNU Radio schematic of an OFDM signal transmission and reception for WiMAX PHY*

Hence, the clipping noise $f(t)$ can be given by

$$f(t) = x(t) - \bar{x}(t) = \sum_{q=1}^{Q} (t) f_q(t) \qquad (13)$$

where Q is the total number of pulses above A. The phase change within a parabolic pulse duration has been studied in [28], and here we directly use these results. The phase variation of $f_q(t)$ from $t = t_q$ to $t = t_q + (\tau_q/2)$ is

$$\Delta\phi_q = \phi\left(t_q + \frac{\tau_q}{2}\right) - \phi(t_q) \simeq \frac{\tau_q}{2}\lambda_q \qquad (14)$$

where

$$\lambda_q = \frac{\dot{x}_I(t_q)}{|x_R(t_q)|} \qquad (15)$$

Here $x_R(t_q)$ and $x_I(t_q)$ denote the real and imaginary parts of $x_t(q)$, respectively, and the dot notation '.' over x_I represents the first derivative computation. The expectation of the absolute value of $\lambda_q \tau_q/2$ is given by

$$E\left\{\left|\frac{\tau_q}{2}\lambda_q\right|\right\} = \frac{\sqrt{\pi}\sigma}{\sqrt{2}A} \operatorname{erfc}\left(\frac{A}{\sqrt{2}\sigma}\right) e^{A^2/2\sigma^2} \qquad (16)$$

where

$$\operatorname{erfc}(x) = 1 - \frac{2}{\sqrt{\pi}} \int_0^x e^{-t^2} \, dt \qquad (17)$$

Equations (14) and (16) lead to an intuitive conclusion that the phase variation $\Delta\phi_q$ in half the pulse duration should be most probably very small (see [28] for a rigid justification). For example $E\{|(\tau_q/2)\lambda_q|\} \simeq 0.03\pi$ when $A/\sqrt{2}\sigma = 2.10$. The analysis above is based on a continuous-time signal, which can be easily extended to a discrete-time case. For a discrete time signal, when the sampling rate is much higher than Nyquist rate, there could be several sample points included in τ_q, where the peak is the sample with the largest amplitude. Evidently, for this case the phase change

between the peak and its adjacent samples is also most probably very small.

From $\bar{x}(n) = x(n) - f(n)$, we know that the amplitude of the clipped signal $\bar{x}(n)$ is not larger than the given threshold value. However, the frequency spectrum of $f(n)$ is distributed over the whole frequency band, and thus $\bar{x}(n)$ exhibits severe out-of-band radiation. Therefore the clipping noise $f(n)$ is not a good choice for the PAPR-reduction vector. To achieve better performance, $f(n)$ requires to be modified: it is out-of-band components need to be ineffective, while its in-band components need to be optimised. Hence, the difference between out-of-band components and in-band components has to be maintained much more (justified in Section 5).

4 System model

A packet has a preamble, header, payload and checksum (typically a CRC value, to validate the packet contents). The preamble is used for detection, synchronisation (in time and frequency) and possibly initial channel state estimation. The header is of fixed length and stores information about the packet, such as (most importantly) its length, but potentially other information, such as the packet number, its intended recipient etc. As shown in Fig. 3, these are modulated and prepared for transmission at the transmitter stage. A GNU schematic is drawn with available signal processing

Table 1 Parameter definition

| Parameters	Values
FFT length (N)	1024
number of occupied tones (N_{used})	896
number of pilots ($P = N/8$)	128
number of data subcarriers (N-P)	768
sampling frequency (f_s)	11.2 MHz
nominal bandwidth	10 MHz
useful symbol time (T_b)	91.4 µs
guard time ($T_g = T_b/8$)	11.4 µs
OFDM symbol duration (T_s)	102.9 µs
subcarrier frequency spacing (Δf)	10.94 µs
digital modulations	BPSK, QPSK, 8PSK, 16QAM, 64QAM, 256QAM.
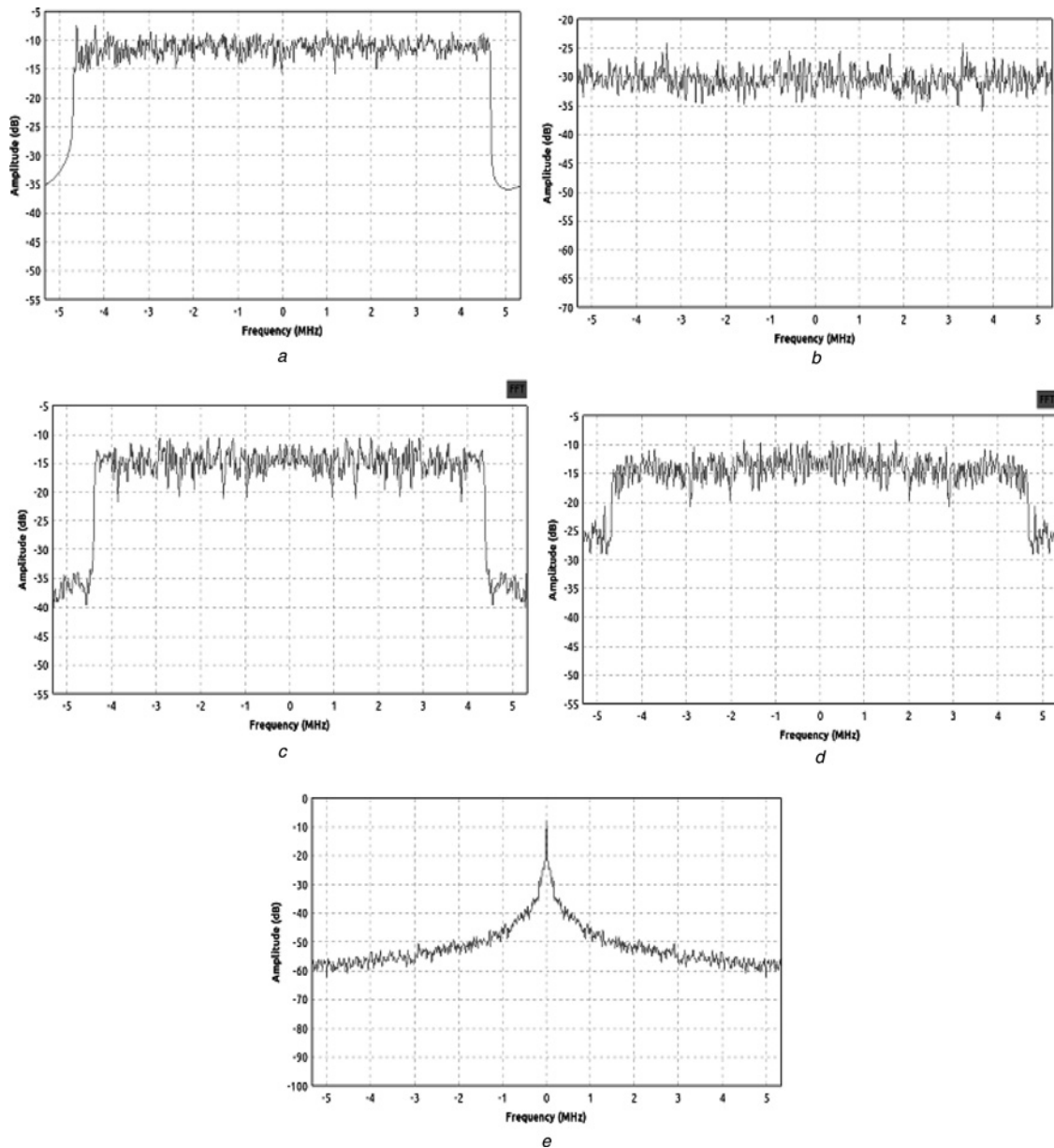
Fig. 8 *Output OFDM spectrum*

a Conventional OFDM
b Phase modulation
c Rail clipping method
d Sample and Hold
e Threshold method

modules for transmitter (Tx) section of OFDM with packet data transmission as shown in Fig. 3.

4.1 Transmitter

It is assumed that the input is a stream of complex scalars with a length tag, that is, the transmitter will work on one frame at a time. The OFDM carrier allocator sorts the incoming complex scalars onto OFDM carriers, and also places the pilot symbols onto the correct positions. Many blocks require knowledge of which carriers are allocated, and whether they carry data or pilot symbols. GNU Radio blocks uses three objects for this, typically called *occupied_carriers* (for the data symbols), *pilot_carriers* and *pilot_symbols* (for the pilot symbols).

Every one of these objects is a vector of vectors. *occupied_carriers* and *pilot_carriers* identify the position within a frame where data and pilot symbols are stored, respectively.

occupied_carriers[0] identifies which carriers are occupied on the first OFDM symbol, *occupied_carriers*[1] does the same on the second OFDM symbol etc.

For example

$$\text{occupied\_carriers} = ((-2, \ -1, \ 1, \ 3), \ (-3, \ -1, \ 1, \ 2))$$

$$\text{pilot\_carriers} = ((-3, \ 2), \ (-2, \ 3))$$

Every OFDM symbol carries four data symbols. On the first OFDM symbol, they are on carriers -2, -1, 1 and 3. Carriers -3 and 2 are not used, hence they are where the pilot symbols can be placed. On the second OFDM symbol, the occupied carriers are -3, -1, 1 and 2. The pilot symbols must be placed elsewhere, and are put on carriers -2 and 3.

If there are more symbols in the OFDM frame than the length of *occupied_carriers* or *pilot_carriers*, they wrap around (in this
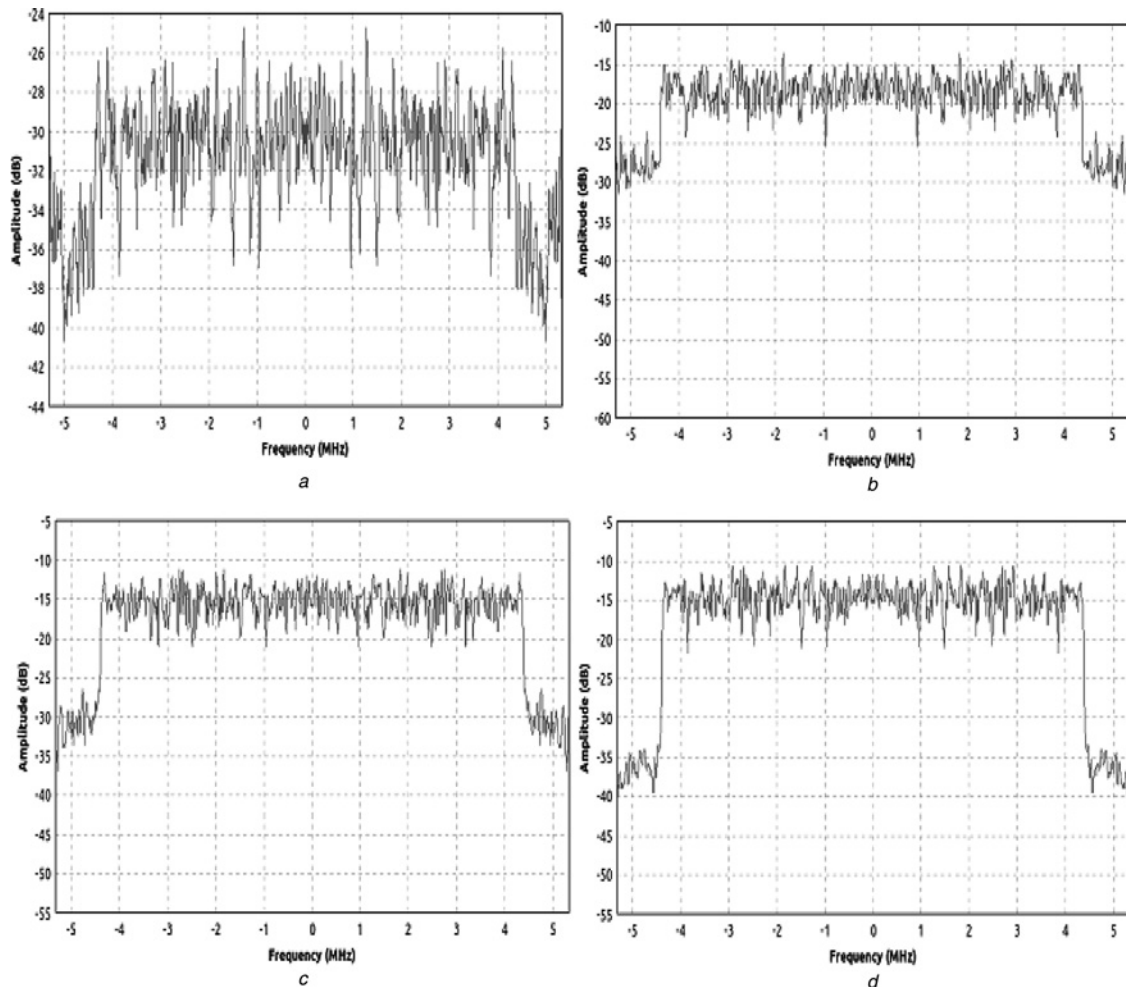
Fig. 9 *FFT plots (frequency domain) obtained for Rail clipping method with threshold level*

a 1
b 5
c 10
d 15

example, the third OFDM symbol uses the allocation in *occupied_carriers*[0]).

The pilot symbols are set by the following valid parameterisation as

$$\text{pilot\_symbols} = ((-1, 1j), (1, -1j), (-1, 1j), (-1j, 1))$$

The position of these symbols are those in *pilot_carriers*. Hence on the first OFDM symbol, carrier −3 will transmit a −1 and carrier 2 will transmit a 1j. We observe that *pilot_symbols* is longer than *pilot_carriers* and the symbols in *pilot_symbols*[2] will be mapped according to *pilot_carriers*[0].

There is also the option to pass OFDM symbols, which are prepended in front of every frame (i.e. preamble symbols). These can be used for detection, synchronisation and channel estimation. These must be converted to time domain signals before continuing, which is why they are piped into an IFFT block. Finally, the cyclic prefix is added to the OFDM symbols and it can also perform pulse shaping on the OFDM symbols (raised cosine peaks in the time domain). Then proposed PAPR reduction techniques are applied on the OFDM symbols and analysed (this point is further illustrated in Section 6). The OFDM symbols with reduced PAPR are passed to the USRP N210 Tx, which converts baseband signal to radio frequency (RF) signal and then transmitted in to air (lab environment).

4.2 Receiver

The transmitted signal is captured by USRP N210 Rx (to synchronise two USRPs, IP addresses are reconfigured) as shown in Fig. 4. The system receives a continuous stream of sample data coming from the USRP N210 Rx device. It discards all the incoming samples until the beginning of a packet is signalled by either a stream tag, or a trigger signal on its second input. An OFDM frame is prepended with a Schmidl and Cox preamble for coarse frequency correction and channel estimation. The fine frequency offset is corrected and that the cyclic prefix is removed. The demultiplexer copies the preamble and header to the first output. The header can then be demodulated with any suitable set of GNU Radio blocks. The data from demux is passed to a block that uses the preambles to perform channel estimation and coarse frequency offset. Both of these values are added to the output stream as tags; the preambles are then removed from the stream and not propagated. Both the coarse frequency offset correction and the equalising (using the initial channel state estimate) are done in the frame equaliser block.

OFDM serialiser is the inverse block to the carrier allocator. It picks the data symbols from the occupied carriers and outputs them as a stream of complex scalars. These can then be directly converted to bits, or passed to a forward error correction (FEC) decoder (If FEC is provided). To turn the information stored in the demodulated header bits into metadata, which can be understood by GNU Radio, a packet header parser block is used to turn the
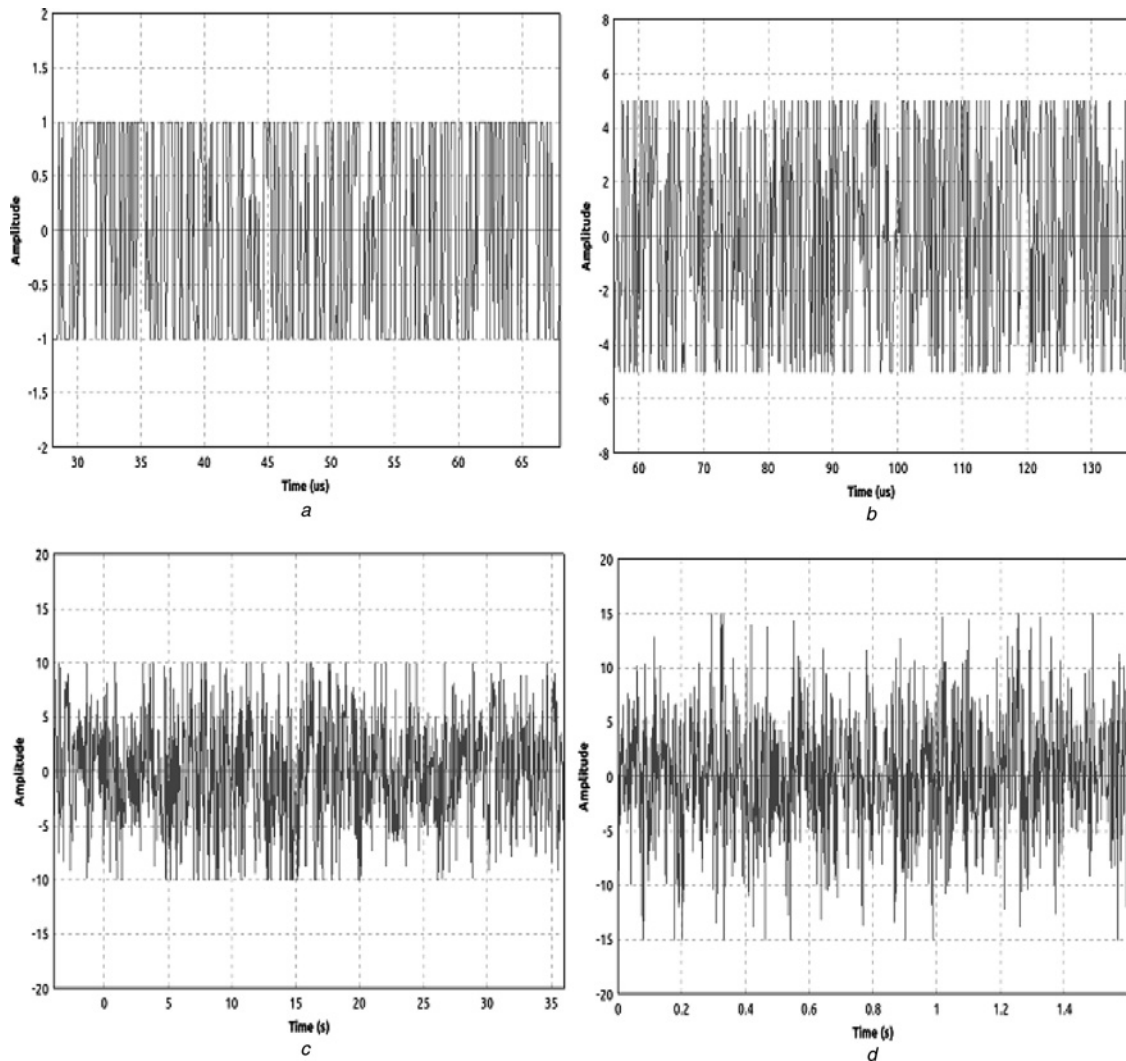
Fig. 10 *Scope plots (time domain) obtained for Rail clipping method with threshold level*
a 1
b 5
c 10
d 15

header data into a message, which is passed back to the header/ payload demuxer. The latter then knows the length of the payload, and passes that out on the second output, along with all the metadata obtained in the header demodulation chain. In Figs. 3 and 4, scope sink and FFT sinks are used to observe the output in time domain and frequency domain, respectively.

5 Experimental results and discussion

The generated conventional OFDM symbol without using any PAPR reduction technique is presented in Fig. 5. The colours in the Fig. 5 show the real and imaginary parts. The high peaks may push the amplifier into the non-linear region that creates many problems that reduce system performance and lead to out of band distortion. To avoid these drawbacks of OFDM systems, the authors of this paper have proposed four PAPR reduction techniques such as phase modulation, rail clipping, sample and hold approach and threshold methods. The motivation behind these techniques is to alleviate the high PAPR and out of band distortion of conventional OFDM system with less complexity. To compare the impact of each technique on the high PAPR OFDM symbol (which shown in Fig. 5) is presented separately in a better layout as shown in Fig. 6. The generated OFDM signal

after using proposed methods has very less PAPR value compared with Fig. 5. In phase modulation method, clipping threshold level is already predefined and it clips according to maximum peak value given. As shown in Fig. 6, phase modulated signal depicts the low peak value and sample and hold output signal has high peak value compared with other known methods. Rail block sets a hard limit on the highest and lowest values at the output of this block. The effect is similar to an operational amplifier that is being driven to saturation (i.e. to the rails). In sample and hold method, when the control input is non-zero, the signal on the in terminal passes to the out terminal. When the control input is zero, the current value on the out terminal is held until the control input is non-zero. Threshold block implements a comparator with configurable hysteresis. The output transitions from 0.0 to 1.0 when the input signal transitions from below to above the high level. The output transitions from 1.0 to 0.0 when the input signal transitions from above to below the low level. The low level must be less than the high level. The obtained low PAPR valued OFDM signal is passed through USRP N210 Tx hardware as shown in Fig. 3. It converts baseband signal to RF signal and transmitted it into air (lab environment). The OFDM signal is received by another USRP N210 Rx hardware and it converts to baseband signal before being processed as shown in Fig. 4.
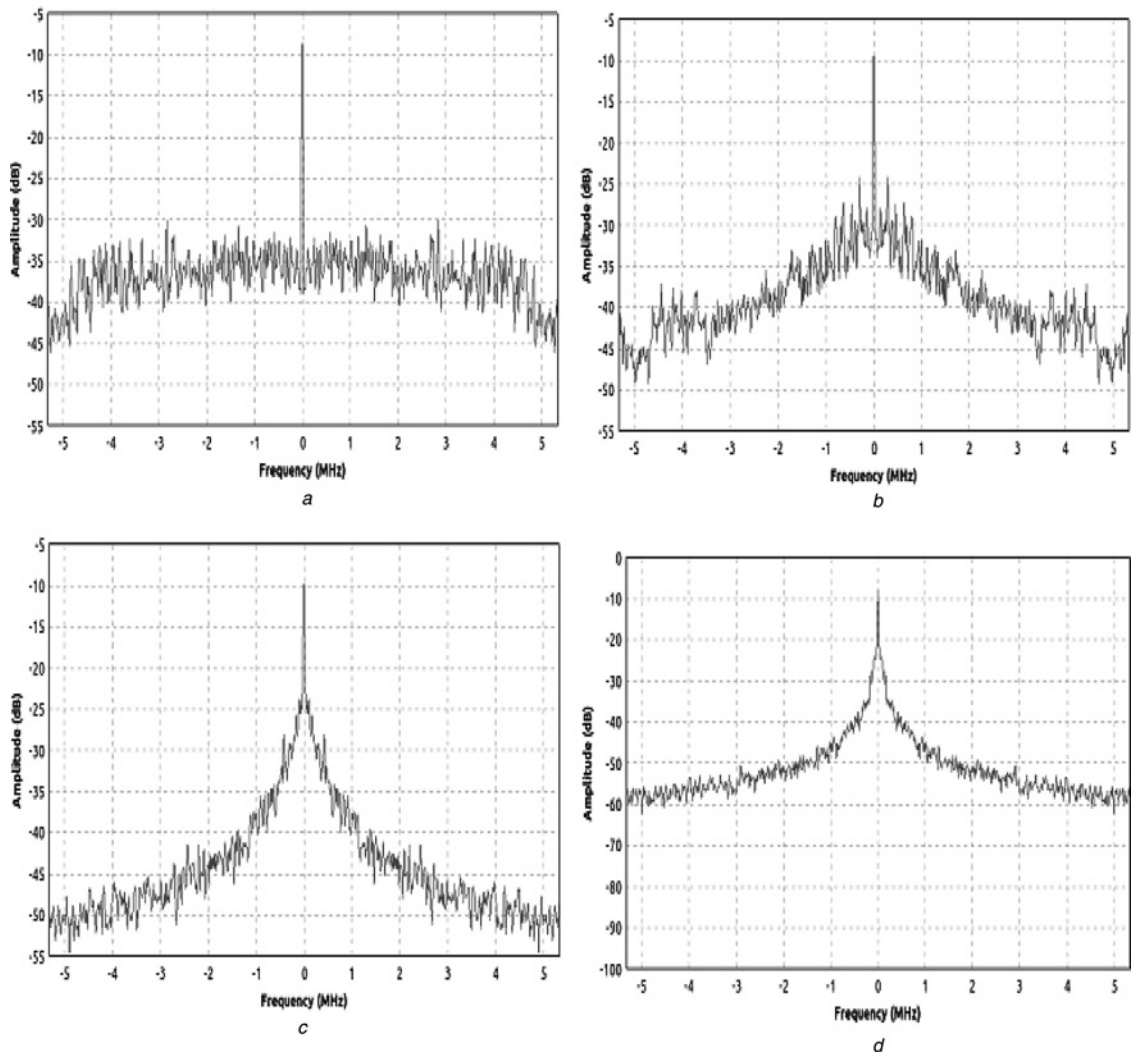
Fig. 11 *FFT plots (frequency domain) obtained for Threshold method with threshold level*
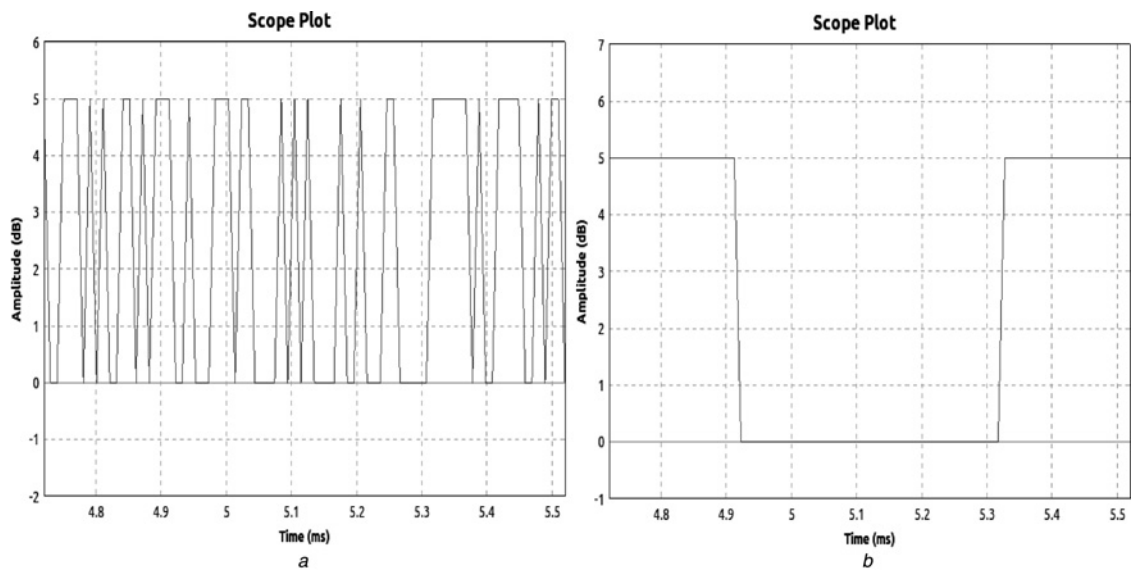
a 1
b 5
c 10
d 15

Fig. 12 *OFDM symbol with reduced PAPR by Threshold clipping method with*

a Threshold level 1
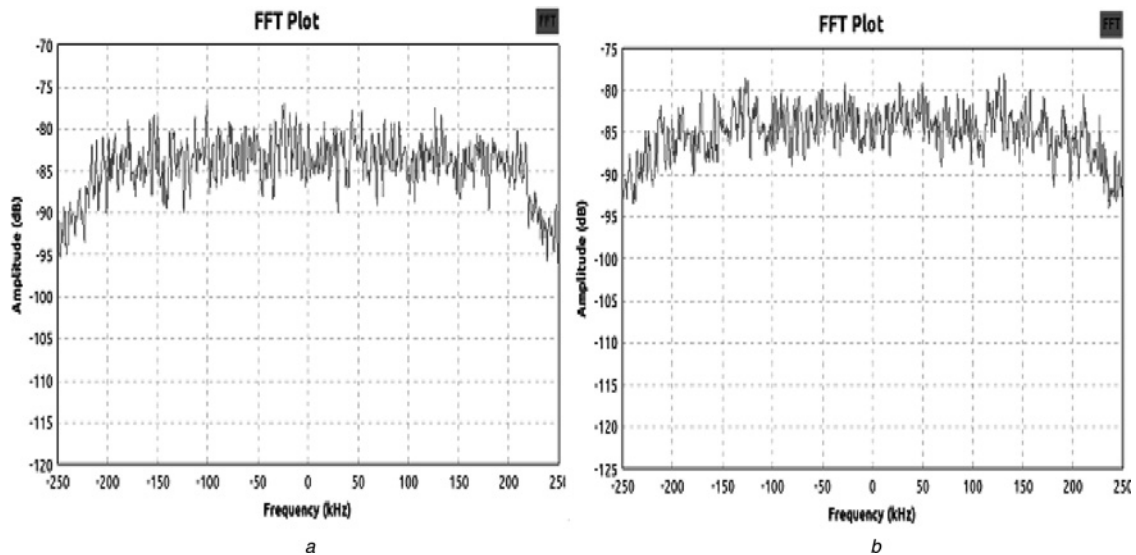*b* Threshold level 10

Fig. 13 *FFT plots obtained by USRP N210 Rx for*

a Without PAPR reduction technique
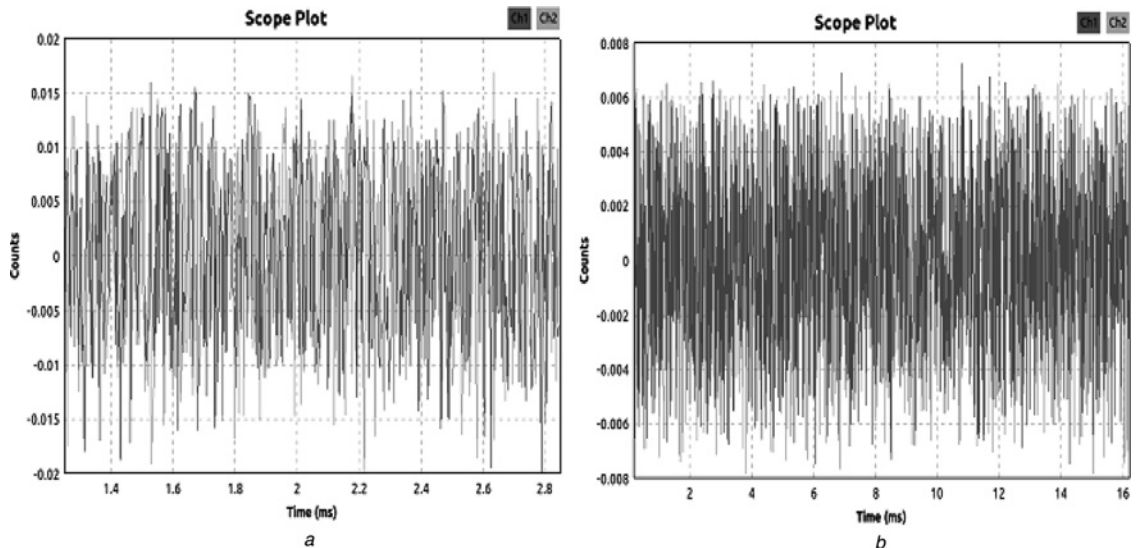*b* With Phase modulation PAPR reduction technique

Fig. 14 *Scope plots obtained by USRP N210 Rx for*

a Without PAPR reduction technique
b With phase modulation PAPR reduction technique

A GNU schematic (signal flow graph) is drawn for analysing the effect of proposed techniques on out of band radiation as shown in Fig. 7. The GNU schematic is drawn as per Mobile-WiMAX specifications [3] which are presented in Table 1. A cosine signal is generated by the use of GNU module 'Signal source' and passed to a scrambler block. The scrambled signal is convolutional coded and then passed to interleaver. The interleaved signal is sent to OFDM block to generate OFDM signals. The OFDM modulated signal might have high peaks and these are reduced by using proposed techniques as shown in Fig. 7. The output OFDM spectra on FFT sinks for proposed methods are shown in Fig. 8. The conventional OFDM (Fig. 8a) has better gap ($\simeq$25 dB) between in-band radiation and out-band radiation. However, the band gap for phase modulation, rail clipping, sample and hold method and threshold methods are $\simeq$1 dB, 30 dB, 15 dB and 50 dB, respectively. The gap between in-band and out-band radiations is analysed by varying clipping threshold value for rail clipping method and threshold methods. The Fig. 9 shows the variation of

out-band distortion for different clipping threshold values using rail clipping method. The band gap for clipping threshold level 1, 5, 10 and 15 are 5 dB, 10 dB, 20 dB and 30 dB, respectively. Hence, it can be concluded from Fig. 9 that the gap between in-band and out-band radiations increases with increment in clipping threshold level. The corresponding time domain waveforms for rail clipping method are shown in Fig. 10. It can be observed that for every one value increment in clipping threshold level, there is a 5 dB increment in the amplitude of OFDM symbol. Hence, threshold value can be reconfigured to the desired level by maintaining out of band radiation also. The Fig. 11 shows the variation of out-band distortion for different clipping threshold values using threshold method. Figs. 12a and b show the spectra for clipping threshold levels of 1 and 10 for threshold block method, respectively. It can be concluded that as clipping threshold level increased, clipping remains the same but the width of signal is increased. The obtained CE-OFDM signal is transmitted to USRP N210 sink that converts baseband signal to

RF signal and sent in to the air. The modulated signal received by USRP N210 source and demodulated accordingly. The demodulated signal can be viewed on scope sink and FFT sink. The OFDM spectrum obtained by USRP N210 Rx for two cases such as conventional OFDM and phase modulated OFDM are shown in Fig. 13. The corresponding time domain waveforms also shown in Fig. 14.

6 Conclusion

In this paper, the wireless transmission of packet data transmission between two USRP N210 s using available GNU modules has been implemented. OFDM based Mobile-WiMAX PHY transmitter and receiver sections are implemented on SDR testbed. The primary drawback of OFDM is high PAPR value and it is mitigated by employing phase modulation, rail clipping, sample and hold approach and threshold method. The experimental results compared original OFDM signal with the proposed methods in terms of PAPR and out-of-band radiation. These simple and low complexity methods brought down the PAPR value to nearly 0 dB and improved the gap between in-band and out-of-band radiations.

7 References

1 Pareit, D., *et al.*: 'The history of WiMAX: A complete survey of the evolution in certification and standardization for IEEE 802.16 and WiMAX', *IEEE Commun. Surv. Tutor.*, 2012, **14**, (4), pp. 1183–1211

2 Tsai, M.-H., Sung, J.-T., Huang, Y.-M.: 'Resource management to increase connection capacity of real-time streaming in mobile WiMAX', *IET Commun.*, 2010, **4**, (9), pp. 1108–1115

3 Khan, M.N., Ghauri, S.: 'The WiMAX 802.16 e physical layer model'. IET Int. Conf. on Wireless, Mobile and Multimedia Networks, 2008, 2008

4 Chang, R.W.: 'Synthesis of band-limited orthogonal signals for multichannel data transmission', *Bell Syst. Tech. J.*, 1966, **45**, pp. 1775–1796

5 Weinstein, S.B., Ebert, P.M.: 'Data transmission by frequency-division multiplexing using the discrete Fourier transform', *IEEE Trans. Commun. Technol.*, 1971, **19**, (5), pp. 628–634

6 Cimini, L.J. Jr.: 'Analysis and simulation of a digital mobile channel using orthogonal frequency division multiplexing', *IEEE Trans. Commun.*, 1985, **33**, (7), pp. 665–675

7 Zou, W.Y., Wu, Y.: 'COFDM: an overview', *IEEE Trans. Broadcast.*, 1995, **41**, (1), pp. 1–8

8 Nee, R. van, Prasad, R.: 'OFDM for wireless multimedia communications' (Artech House, Inc., 2000)

9 Shepherd, S., Orriss, J., Barton, S.: 'Asymptotic limits in peak envelope power reduction by redundant coding in orthogonal frequency division multiplex modulation', *IEEE Trans. Commun.*, 1998, **46**, (1), pp. 5–10

10 Ochiai, H., Imai, H.: 'On the distribution of the peak-to-average power ratio in OFDM signals', *IEEE Trans. Commun.*, 2001, **49**, (2), pp. 282–289

11 Thompson, S.C.: 'Constant envelope OFDM phase modulation'. PhD. dissertation, University of California, San Diego, 2005. [Online]. Available: http://elsteve.com/thesis/

12 Sabbaghian, M., Kwak, Y., Smida, B., Tarokh, V.: 'Near Shannon limit and low peak to average power ratio turbo block coded OFDM', *IEEE Trans. Commun.*, 2011, **59**, (8), pp. 2042–2045

13 Urban, J., Marsalek, R.: 'OFDM PAPR reduction by combination of Interleaving with Repeated clipping and filtering'. 14th Int. Workshop on Systems, Signals and Image Processing, 2007, pp. 249–252

14 Cha, S., Park, M., Lee, S., Bang, K.-J., Hong, D.: 'A new PAPR reduction technique for OFDM systems using advanced peak windowing method', *IEEE Trans. Consum. Electron.*, 2008, **54**, (2), pp. 405–410

15 Hou, J., Ge, J., Li, J.: 'Peak-to-average power ratio reduction of OFDM signals using PTS scheme with low computational complexity', *IEEE Trans. Broadcast.*, 2011, **57**, (1), pp. 143–148

16 Ghassemi, A., Gulliver, T.A.: 'PAPR reduction of OFDM using PTS and error-correcting code subblocking-Transactions Papers', *IEEE Trans. Wirel. Commun.*, 2010, **9**, (3), pp. 980–989

17 Jiang, T., Wu, Y.: 'An overview: peak-to-average power ratio reduction techniques for OFDM signals', *IEEE Trans. Broadcast.*, 2008, **54**, (2), pp. 257–268

18 Armstrong, J.: 'Peak-to-average power reduction for OFDM by repeated clipping and frequency domain filtering', *IEE Electron. Lett.*, 2002, **38**, (5), pp. 246–247

19 Wang, Y.-C., Luo, Z.-Q.: 'Optimized iterative clipping and filtering for PAPR reduction of OFDM signals', *IEEE Trans. Commun.*, 2011, **59**, (1), pp. 33–37

20 GNU Radio: 'The GNU Radio Companion', 2012. [online]. Available at http://www.ece.uvic.ca/elec350/grc_doc/ar01s01.html

21 Ettus Research, USRP N210 (2012). Available at https://www.ettus.com/product/details/UN210-KIT. Accessed 08 February 2014

22 Mitola, J.: 'The software radio architecture', *IEEE Commun. Mag.*, 1995, **33**, (5), pp. 26–38

23 Jondral, F.K.: 'Software-defined radio: basics and evolution to cognitive radio', *EURASIP J. Wirel. Commun. Netw.*, 2005, pp. 275–283

24 Reis, G., Luiz, A.: 'Introduction to the Software-defined Radio Approach', *IEEE Latin Am. Trans.*, 2012, **10**, (1), pp. 1156–1161

25 GNU Radio: 'The gnu software radio', 2007 [online]. Available at https://gnuradio.org

26 Dahlman, E., Parkvall, S., Skold, J.: '4G: LTE/LTE-advanced for mobile broadband' (Academic Press, 2013)

27 Jiang, T., Guizani, M., Chen, H.S., Xiang, W.D., Wu, Y.Y.: 'Derivation of PAPR distribution for OFDM wireless systems based on extreme value theory', *IEEE Trans. Wirel. Commun.*, 2008, **7**, (4), pp. 1298–1305

28 Wang, L., Tellambura, C.: 'Analysis of clipping noise and tone reservation algorithms for peak reduction in OFDM systems', *IEEE Trans. Veh. Technol.*, 2008, **57**, (3), pp. 1675–1694